1. Introduction

The electrocardiogram (ECG) is a powerful tool used by clinicians that measures the electrical depolarization of the heart. It is most often used to identify cardiac structure and function. Yet deeper analysis of ECGs can also be used to consider more in depth physiological topics - ranging from heart rate detection, to measuring the electrical axis of the heart.

Unfortunately, there are a variety of complications that can make the ECG data less accurate and difficult use in physiological analysis. Aliasing – which is caused by digitally sampling analog signals at an inappropriately low rate – misrepresents high frequency components as lower frequencies. Noise can also convolute a signal, making it difficult to identify peaks. Common sources of noise vary – examples include high frequency biological signals from muscles, 60 Hz noise from surrounding electronics and low frequency drift from breathing.

Appropriate equipment setup and analysis techniques can prevent aliasing and reduce the presence of noise – allowing us to extract useful biological data. Examples of such design changes include sampling rate and filter settings. Therefore, this study focused on establishing such methods for maximizing the quality of information obtained from raw ECG signals.

With optimal settings determined, it is then possible to gather more meaningful biological data. In this report, low pass filter optimization was applied for use in two physiological studies: the effect of exercise and the Valsalva maneuver (exhaling while mouth and nose are closed) on heart rate, and measuring the mean QRS axis of the heart.

2. Materials and Methods

The apparatus for collecting ECG's consisted of the following: silver-silver chloride ECG electrodes (GE Medical Systems Silver Mactrode Plus Model E9001AD / Dymedix Dual Electrode Model 5200-0001) placed on the two wrists and left ankle, a differential amplifier (Isodam Biological B), an isolation amplifier (Texas Instruments ISO122) and a data acquisition (DAQ) board (Data Translation DT9804). (Figure 1).

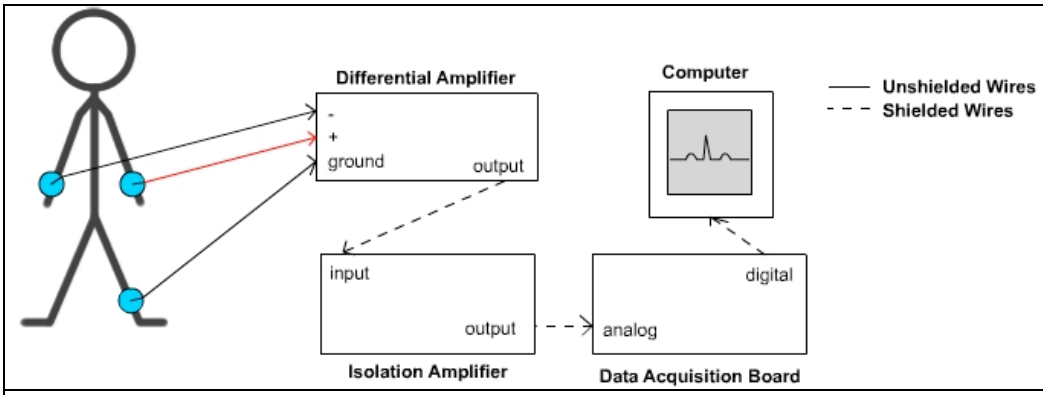

Figure 1. Instrument setup for ECG recording.
The ECG recording setup started with three electrodes placed on the subject. The signal was transmitted to a differential amplifier via unshielded alligator clips; the output was then sent to an isolation amplifier via shielded BNC cables. Next, the signal was transmitted to a data acquisition board which converted the analog signal into a digital representation. Ultimately, the signal was read and stored by a computer, which reconstructed the signal.

Prior to ECG recordings, the frequency response of the isolation amplifier was determined using a function generator (Wavetek). The difference of input (11.05 V) and output signal amplitude was measured on an oscilloscope (Hewlett Packard S4603B) as a function of frequency (which was varied from 0.65 Hz – 2.35 kHz).

Aliasing effects were observed with the DAQ board by comparing input frequency (10-200 Hz signals from the Wavetek) and post-sampling observed frequencies using a 100 Hz sampling rate.

When taking ECGs, the skin was abraded with an alcohol wipe prior to attaching electrodes to reduce resistance. Raw ECGs were collected using 1000x gain (to amplify the ~ 1 mV signal without saturation) and 0.1 – 200 Hz pass filter settings (to reduce noise above 200

Hz - the upper limit of ECG frequencies) on the differential amplifier. ECGs taken at various sampling rates (30 Hz-1 kHz), were analyzed to determine an appropriate ECG sampling rate, which was subsequently used on all recordings.

Fourth order Butterworth filters (58-62 Hz bandstop, 5 Hz low pass, 30 Hz low pass, 0.2 Hz high pass) were used to identify the effect of filtering on raw ECG data. Power density spectra (PDS, calculated with a Welch algorithm, Nfft = window = 1024, overlap = 512), were used to analyze the effectiveness of these filters.

A noise reduction and signal intensity quantification (NRSIQ) algorithm was developed in MATLAB for optimizing low pass filters. This program applied digital filters and objectively analyzed two characteristic of the resulting signal: attenuation of the QRS and amount of noise remaining. The QRS attenuation was quantified by the difference in the signal's absolute maximum and minimum. Noise was quantified as the area between the curve that connects all local maxima, and the curve that connects all local minima. (Figure 2). How the low-pass cutoff frequency (defined throughout this paper as -3 dB) affected QRS attenuation and amount of noise remaining were used to select optimal filter settings for the physiological measurements.

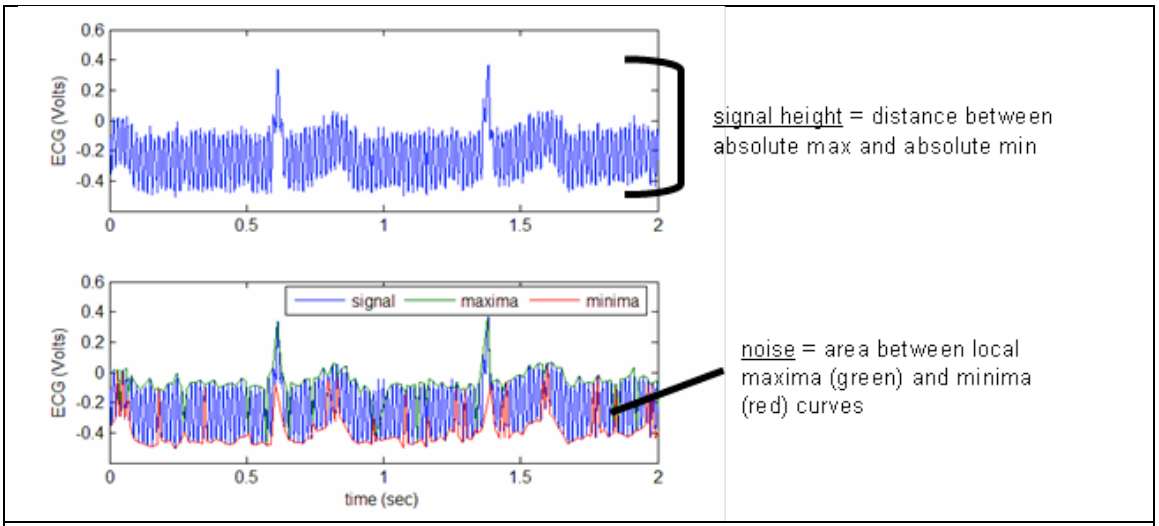

Figure 2. Noise reduction and signal intensity quantification (NRSIQ) algorithm.
The first graph indicates how QRS height was measured. In the NRSIQ algorithm, QRS height was found by taking the difference between the signal's absolute maximum and minimum. The second graph indicates how the signal noise was quantified. All local maxima were connected (green line) and all local minima were connected (red line). The amount of high frequency noise was then measured as the area defined between the green and red lines.

ECGs of two subjects were taken at rest and after exercise (running five flights of stairs). ECGs of one subject was recorded while performing the Valsalva maneuver. A peak detection algorithm and heart rate calculator was scripted in MATLAB using the Hamliton and Tompkins method. Fourth order Butterworth filters with optimal settings found by the NRSIQ method (58-62 bandstop, 20 Hz cutoff lowpass) were used prior to differentiating. A 1-10 Hz bandpass filter was ultimately used to smooth the final curve on which peaks were detected as local maxima.

The axis of the heart depolarization was measured by recording two simultaneous ECGs and using vector projection geometry to solve for magnitude and angle (Figure 3). Raw ECGs were filtered using NRSIQ optimal 1000th order least-squares filters (58-62 bandstop, 30 Hz cutoff lowpass). Least square filters were used (rather than Butterworth) because they are linear phase filters and will not distort the shape of the signal. To find the mean angle of the QRS complex, the mean QRS axes from multiple cardiac cycles were averaged.

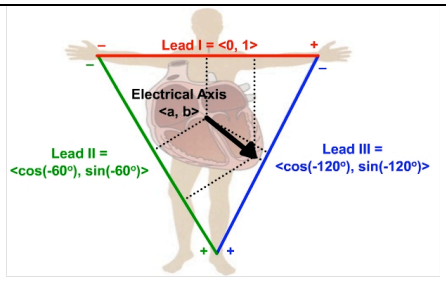

$ECG_{LeadI} = \langle a, b \rangle \bullet \langle 1, 0 \rangle$
$ECG_{LeadII} = \langle a, b \rangle \bullet \langle \cos(-60^{o}), \sin(-60^{o}) \rangle$
$ECG_{LeadIII} = \langle a, b \rangle \bullet \langle \cos(-120^{o}), \sin(-120^{o}) \rangle$

Figure 3. Methods used in calculating electrical axis of the heart. The *magnitude and angle of the electrical axis can be calculated from any two simultaneous leads. This is because measured leads are the projection of the electrical axis onto the lead unit vectors. Vector geometry provides the three equations listed above, each having two unknowns. Manipulating two of the equations with ECG data from two leads allows for both the magnitude and angle to be calculated.*

3. Results

3.1. Frequency Response of the Isolation Amplifier

The isolation amplifier showed no decrease in signal amplitude with varying frequency (Figure 4). The ratio of output voltage to input voltage (V_o/V_i) was calculated to be approximately 0 ± 0.3 dB for all frequencies tested between 0.65 Hz and 2.35 kHz

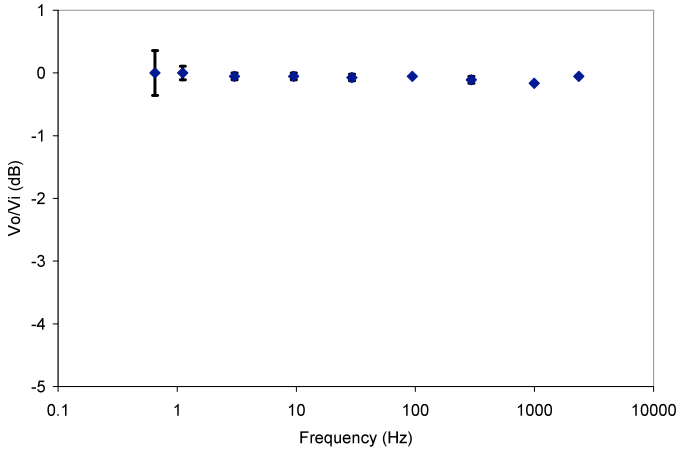

Figure 4. Frequency response of isolation amplifier.
There is no significant amplitude attenuation for all frequencies between 0.65 Hz and 2.35 kHz. Since ECG frequency components usually fall close to within this range, the isolation amplifier is deemed adequate for use in ECG recordings. These results show that certain frequencies of an ECG will not be preferentially amplified.

3.2 Effect of Sampling Rate on Signal Collection

The relationship between inputted frequency and apparent frequency showed a triangular wave pattern (Figure 5) with period equal to the sampling rate (100 Hz) and height equal to one half the sampling rate, also referred to as the Nyquist frequency (50 Hz). A model was fit to the data (Equation 1).

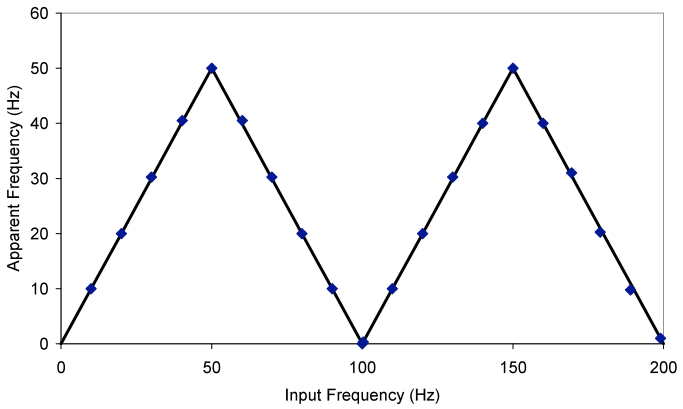

Figure 5. Alias effect caused by low sampling rates.
Sinusoids of varying input frequency were recorded with a 100 Hz sampling rate. High frequencies appear lower after sampling, due to an inadequate sampling rate. The triangular pattern is typically of the "folding back" phenomenon of aliasing. The period of this wave is equal to the sampling rate, and the amplitude is equal to the Nyquist frequency (one half the sampling rate, or 50 Hz). A model fitted to the data (Equation 1) can be used to predict apparent frequencies from the input frequency and Nyquist frequency.

$$f_a = \left(\left\lfloor \frac{f}{f_N} \right\rfloor \equiv 2\right) * \left(f_N - f \equiv f_N\right) + \left(1 - \left\lfloor \frac{f}{f_N} \right\rfloor \equiv 2\right) * \left(f \equiv f_N\right) \quad (1)$$

Where: $\lfloor a \rfloor$ designates the highest integer lower than a

$a \equiv b$ designates a modulo b

f_a = apparent frequency, f = inputted frequency, f_N = Nyquist frequency

ECGs showed distortion when sampled at low rates (Figure 6). At 30 Hz sampling rate, the height of the QRS was irregular. Sampling at higher rates restored the original signal shape pf the ECG (as measured on an oscilloscope with a high sampling rate of 20 MHz).

3.3. Collection of ECGs and Effect of Filtering

A typical raw ECG signal can be found in Figure 7a. Prominent R and T waves are distinguishable. However, these raw data plots have a considerable amount of high frequency noise and low frequency drift that mask the presence of the P and Q waves. The PDS for these raw ECGs (Figure 7b for typical PDS, Welch method, window length of 1.024 seconds) show

spikes of power at 60, 120, 180, (etc.) Hz. The PDS also shows that most ECG data is present at frequencies below 50 Hz (most frequencies higher than 50 Hz have amplitudes of less than –50 dB, except the 60 Hz noise peak).

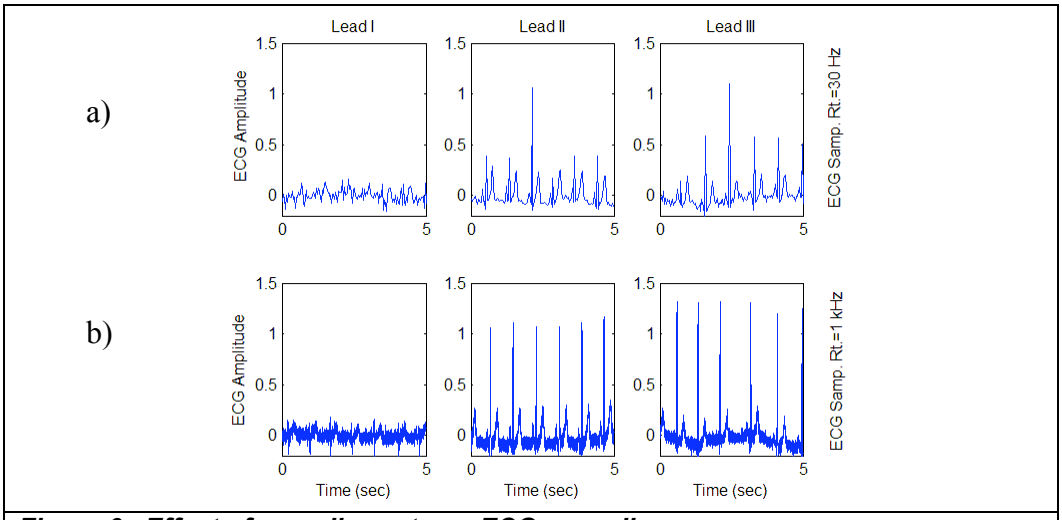

Figure 6. Effect of sampling rate on ECG recordings.
a) ECGs at a sampling rate of 30 Hz (top row) show distortion of the true signal. The R wave has been irregularly shorted in all three leads due to aliasing.
B) However, increasing the sampling rate to 1kHz restored the ECG to it original shape (as measured on the oscilloscope). A sampling rate of 1 kHz is therefore preferable.

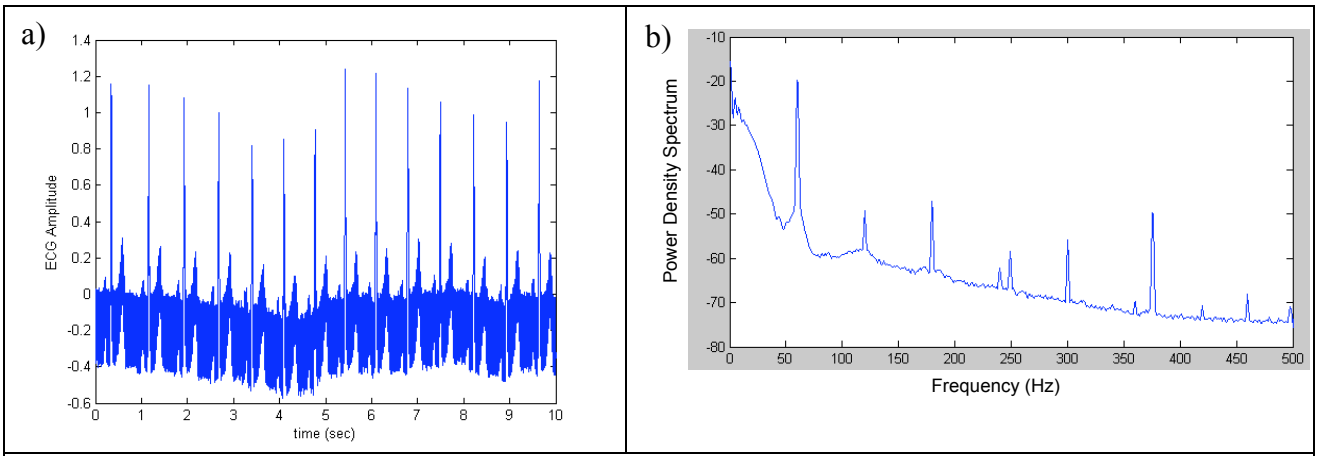

Figure 7. Lead II: Raw ECG signal and corresponding power density spectrum (PDS).
a) Selected portion of ECG. A large amount of high frequency noise can be seen in the raw ECG signal. Low frequency drift can be seen by the unsteady baseline.
b) The correpsonding PDS (confirms the prescence of noise. Large amounts of noise can be seen at 60 Hz and its harmonics. Because most of the signal power lies under 50 Hz, all frequencies greater than 50 Hz were believe to be noise as well.

Use of a fourth order Butterworth 60 Hz bandstop filter made the ECG considerably less noisy (Figure 8a) and removed the 60 Hz peak on the PDS (Figure 8b). An additional fourth order Butterworth 30 Hz low pass filter removed high frequency noise (Figure 9) and produces a clean signal with little drift. Lowering the cut-off frequency of the low pass filter to 5 Hz instead of 30 Hz, however, resulted in significant distortions of the signal. Rather than one distinct R wave, there were two sharp peaks (Figure 10). All attempts to use a high pass filter to remove drift failed; instead of removing drift, the interval between the T an P waves became highly curve (compared to a flat line typical in model ECGs). (See Figure 11).

3.4. Optimization of High Pass Filter Settings

The NRSIQ algorithm (Figure 2) produced plots that can be used to determine optimal cut off frequency for low pass filters. QRS height and signal noise are shown as functions of the cutoff frequency (Figures 12). All NRSIQ plots show similar trends: a decrease in cutoff frequency corresponds to a decrease in QRS height and a decrease in signal noise

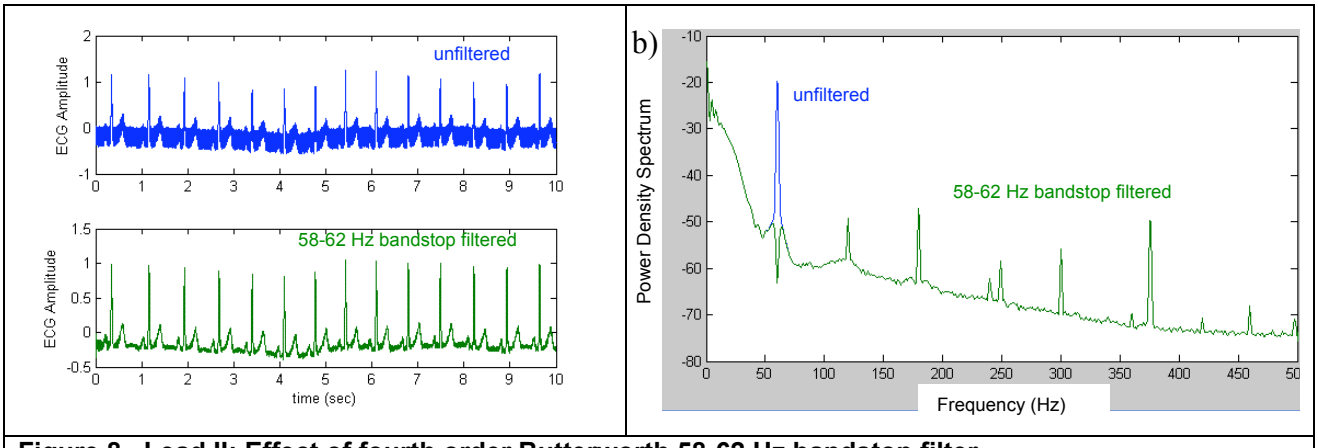

Figure 8. Lead II: Effect of fourth order Butterworth 58-62 Hz bandstop filter.
a) Application of the bandpass filter around 60 Hz reduced a significant amount of noise from the signal. However, there is still some high frequency noise present.
b) The PDS also shows the loss of 60 Hz noise. As seen in the signal, there is still some high frequency noise present.

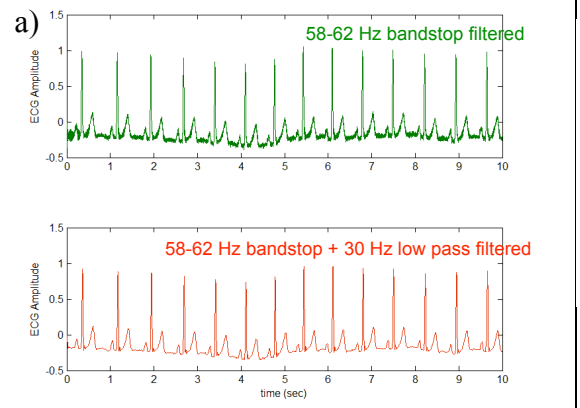

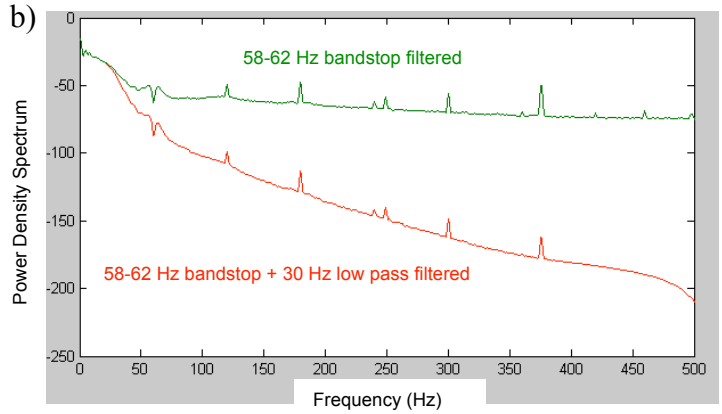

Figure 9. Lead II: Effect of fourth order Butterworth 30 Hz low pass filter.
a) The additional application of the 30 Hz low pass filter reduced almost all high frequency noise in the signal. There is still mild drift present, but the signal is very clear.
b) The PDS also shows the loss of high frequencies. Above 50 Hz, the power density is no greater than -75 dB.

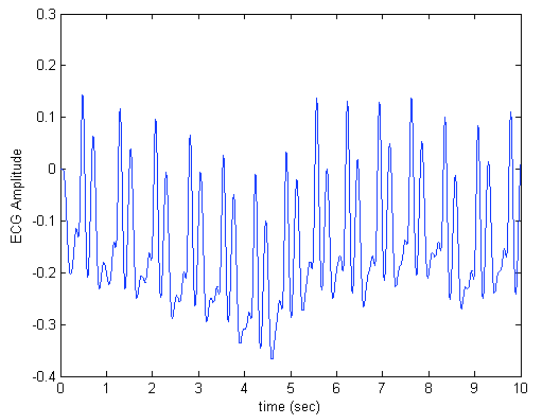

Figure 10. Lead II: Effect of fourth order Butterworth 5 Hz low pass filter.
A low pass filter has the ability to remove high frequency noise from an ECG signal. However, choice of cut-off frequency is important. Choosing one too low can cause distortion of the signal. This is what has occurred in the figure. The signal above has almost no indication of the original ECG signal.

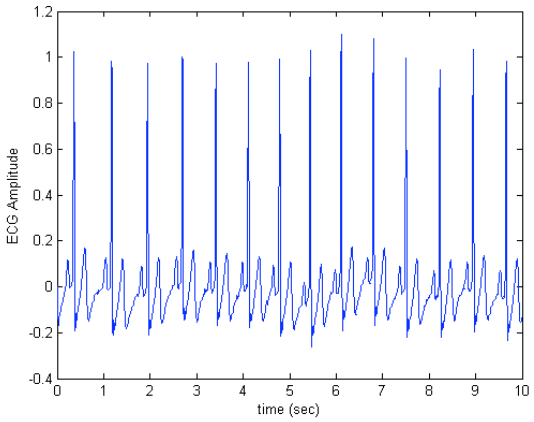

Figure 11. Attempt to remove drift with a fourth order Butterworth 0.2 Hz high pass filter.
All attempts to remove drift from the ECG were not successful. Rather than removing drift, the high pass filters distorted the T-P interval of the ECG – making any analysis conducted erroneous.

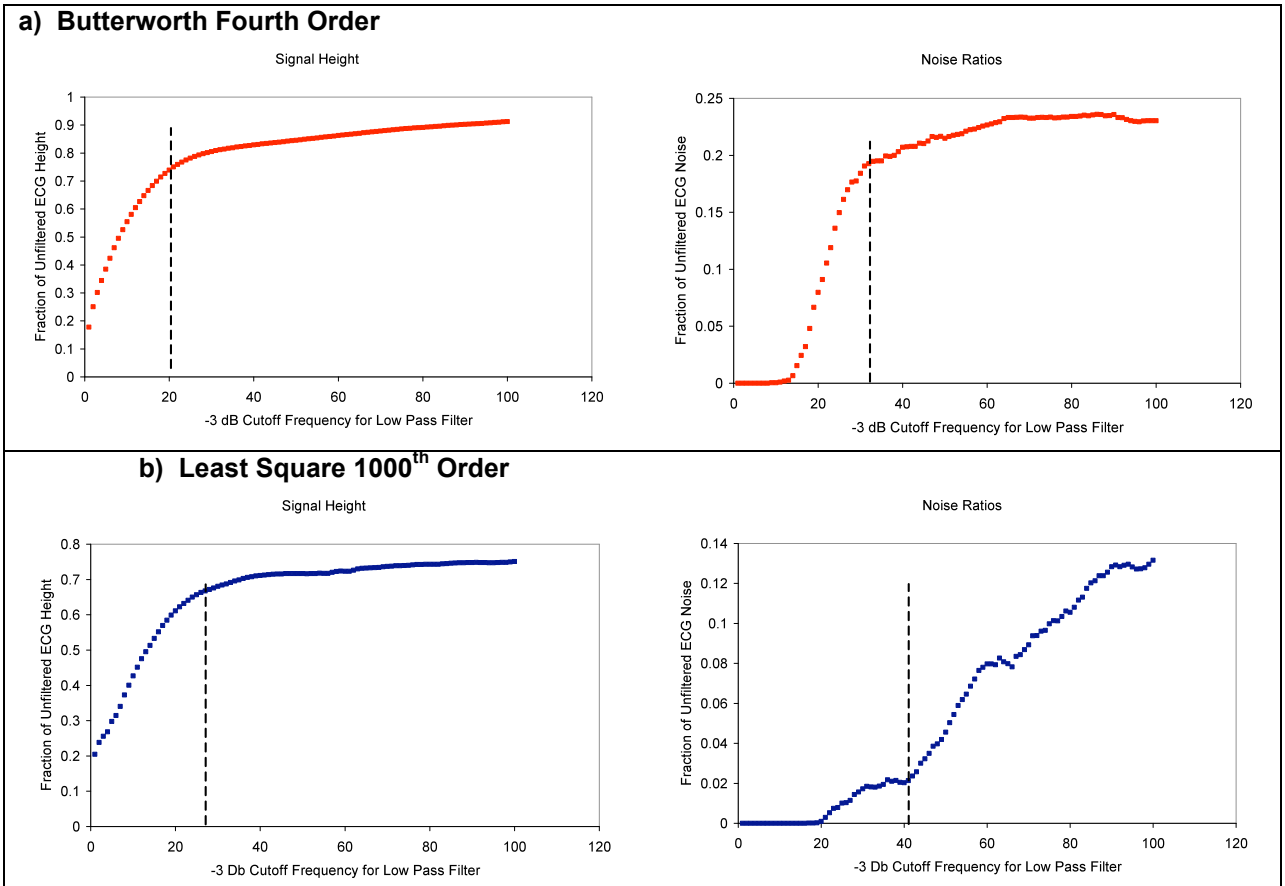

Figure 12. Examples of NRSIQ algorithm: QRS height and signal noise plots as a function of -3 dB cutoff frequency.
Average of all three leads. Calculated after 58-62 bandstop was applied.
a) Fourth order Butterworth NRSIQ plots are shown. The graph on the left plots the height of the QRS as a function of -3 dB cutoff frequency. The height is represented as the fraction of the unfiltered signal's original height. This graph shows that QRS height starts to significantly attenuate as cut off frequency approaches 20 Hz. The right graph shows the amount of noise remaining in the signal as a function of cutoff frequency. Noise does not start to significantly decrease until the cut off approaches 30 Hz.
b) 1000th order least squares NRSIQ plots are shown. Similar to the Butterworth Graphs, the left graph shows QRS height as a function of cutoff frequency. The QRS does not begin to significantly attenuate until a cutoff frequency of 30 Hz. However, the noise remaining graph shows that a significant amount of noise has been removed for any cut off frequency less than 40 Hz.

3.5 Physiological ECGs

3.5.1. Heart Rate Detection

The Hamilton and Tompkins peak detection algorithm (Appendix A) reliably identified all QRS peaks (100%, n=798) in a 10-minute ECG. There were zero false positives. The mean heart rate for the trial was 79.0 ± 0.3 beats per minutes (bpm).

The PDS (Welch method, window length of 1.09 minutes) was also analyzed for the 10-minute ECG (Figure 13). The fundamental peak corresponding to the heart rate was identified at 1.33 ± 0.0075 Hz, corresponding to 79.7 ± 0.45 bpm. A t-test between the peak detection mean heart rate and PDS calculated heart rate produced a p-value of 1.43×10^{-5}, indicating that the mean heart rates are statistically different.

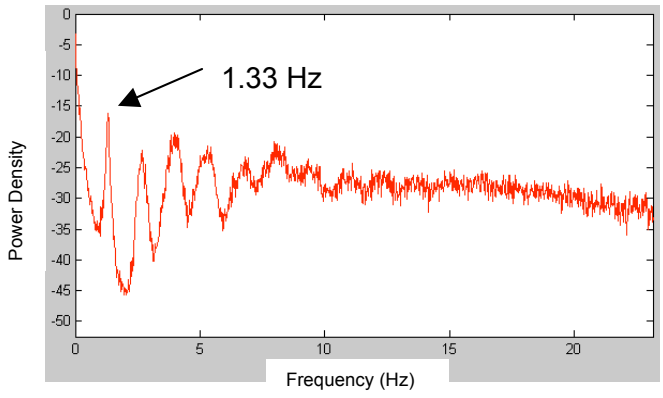

Figure 13. Fundamental peak of 10 minute ECG.
The fundamental peak corresponding to heart rate was identified as 1.33 Hz for a 10 minute ECG run. This value correlates to a heart rate of 79.7 bpm.

The error for the PDS heart rate value (0.015 Hz, corresponding to 0.9 bpm) was calculated as one half the PDS frequency resolution. The resolution was calculated from the window length chosen for Welch PDS analysis. A 1.09 minute (65.4 sec) window allows for a minimum of 0.015 Hz (1/65.4 sec) to be detected.

3.5.2. Effect of Activity on Heart Rate

The at-rest heart rates for two subjects were 86.6 ± 1.1 bpm and 82.3 ± 1.3 bpm. Exercise caused the heart rates of both subjects to increase to 139.0 ± 1.5 bpm and 129.9 ± 1.4 bpm respectively. P values for t-tests comparing the rest and after-exercise heart rates were approximately 0 for both subjects, indicating there is a statistically significant difference between heart rates during the two activities.

The Valsalva maneuver was performed by a single subject five times. The characteristic shape of the graph included: a sharp decrease in heart rate within the first ten seconds, and then a sustained high heart rate until the maneuver ceased (figure 14). The heart rate dropped to 63.1 ± 2.6 bpm within the first ten seconds, while it rose to a sustained high heart rate of 104.3 ± 3.3 bpm.

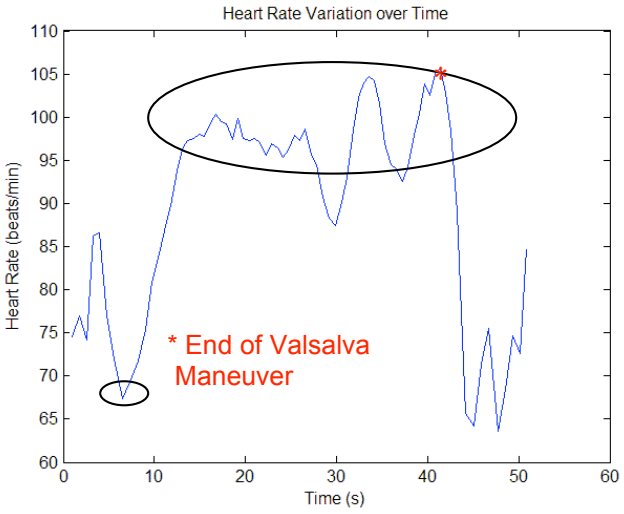

Figure 14. Characteristic variation in heart rate while performing Valsalva maneuver.
A subject perfomed the Valsalva maneuver 5 times. All showed a characteristic heart rate variation over time. Within 10 seconds of the start of the maneuver, heart rate dropped from a normal value of ~80 bpm to 63.0 ± 2.6 bpm. Heart rate then increases dramatically and plateaued until the maneuver ceased. The heart rate peaked at 104.2 ± 3.3 bpm.

3.5.3. Calculating Electrical Axis of the Heart

Mean axis during the QRS was also calculated for each lead combination, as well as an average of all lead combinations (See Table 1). Average QRS axis was 55.1 ± 0.8 bpm for subject one. The average QRS axis was 53.6 ± 0.5 for subject two. An ANOVA test showed that the three lead combinations (I/II, I/III, II/III) are not equivalent in calculating mean QRS axis for both subjects (p-values were approximately 0).

Table 1. Summary of mean QRS electrical axes data.

	Subject 1 Mean QRS (^{o})	Subject 2 Mean QRS (^{o})
Leads I and II	**50.8 ± 1.7**	**53.2 ± 0.5**
Leads I and II	**55.2 ± 1.4**	**51.9 ± 1.1**
Leads I and II	**58.4 ± 1.1**	**55.8 ± 0.9**
Average	**55.1 ± 0.8**	**53.6 ± 0.5**
ANOVA Score (H_0: $\mu_1=\mu_2=\mu_3$)	**~0**	**~ 0**

4. Discussion

4.1. Frequency Response of Isolation Amplifier

All frequencies tested (0.65 Hz and 2.35 kHz) in the frequency response of the isolation amplifier showed no difference between output and input amplitudes (V_o/V_i = 0 dB) (Figure 4). Because most frequencies of the ECG fall within the range tested, the isolation amplifier can be considered sufficient to use in all testing detailed in this report. It should not preferentially amplify any specific frequency component of the ECG signal.

4.2. Aliasing and Its Impact on Choosing Sampling Rate

Sampling rate is an important parameter that must be optimized when collecting ECGs. The importance of choosing an appropriate sampling rate can be seen in Figure 5 . When the frequency of the inputted sine wave was higher than the Nyquist frequency (50 Hz for this specific trial), the signal became distorted. High frequency signals (>50 Hz) appeared as low frequency signals (<50 Hz) due to the inability of low sampling rates to probe every period of a wave twice (See figure 15). The result (aliasing) is a misrepresentation of the original frequency in a systematic manner shown in figure 5. This phenomenon of “folding back” can be seen as a triangle wave in the graph, and provides a model (Equation 1) for predicting apparent frequency at any input frequency. This formula allows the prediction of apparent frequencies for any input frequency, such as 500, 525 and 550 Hz. Apparent frequencies for 500, 525 and 550 Hz were calculated using the equation and confirmed via experimentation to be 0, 25 and 50 ± 0.8 Hz respectively.

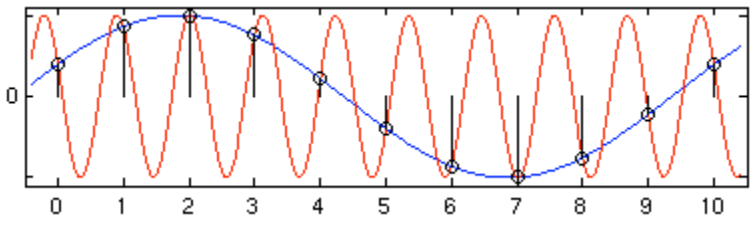

Figure 15. Example of how aliasing occurs when low sampling rate is chosen.
Aliasing is due to inability of low sampling rates to probe every period of a wave twice .

In order to prevent the loss of data associated with aliasing, high sampling rates must be used. Distortion of the signal begins when input frequencies are above the Nyquist frequency. As a rule, the sampling rate for all experiments should be set to at least two times faster than the frequency of the signal.

Aliasing can significantly affect complex signals such as ECGs. Because all complex periodic signals are made up of a sum of purely sinusoidal waves, high frequency components can become aliased if the sampling rate is not chosen high enough. The result is distortion of the true signal – similar to that of a low pass filter. This can be seen when comparing the ECGs sampled with 30 Hz and 1 kHz (Figure 6). The ECG sampled at 30 Hz does not accurately nor consistently report the height of the QRS complex. The high frequencies in the QRS have been folded back to lower frequencies. Care must be taken to pick a sampling rate high enough to prevent such effects. Given that the maximum frequency of an EKG is approximately 150 Hz, a sampling rate of at least 300 Hz is suggested. A sampling rate of 1 kHz was used in all experiments discussed within this report, to provide additional room to prevent aliasing.

4.3. Analysis of Raw ECG Signals and Effect of Filtering

With an appropriately set sampling rate (1 kHz), ECGs were collected (See Figure 7 for typical data set). Compared to ECGs previously reported in the literature, these signals showed considerable amounts of high frequency noise. While the R and T waves are noticeable, the P and Q waves are not. Furthermore, there is low frequency drift that distorts

what should be a stable baseline. It is undesirable to leave the ECG signals in this form because they are much more difficult to use. Clinically, the inability to see P-waves can prevent proper diagnosis of atrial defects. Experimentally, it can prevent amplitudes from being properly subtracted when calculating the mean axis of the heart. Therefore, removal of noise from the raw signals is strongly needed.

The necessity of filtering is confirmed when the PDS is analyzed (Figure 7b). The peaks found at the multiples of 60 Hz most likely correspond to 60-Hz noise and its harmonics. Our system is especially susceptible to 60 Hz noise from surrounding electronics because wires used to connect the subject and Isodam amplifier were not shielded. In the future, the use of shielded wires may decrease 60 Hz noise and is recommended. However, it is unlikely to remove all 60 Hz noise from the signal.

Aside from 60 Hz resonance peaks, there is other noise noticeable in the PDS (Figure 7b). Most of the power in the ECGs is located below 50 Hz, and therefore higher frequencies in this scan are most likely noise as well. This noise probably has a wide variety of sources. On may be the changing electrical potential of muscle cell membranes. In the literature, surface electrodes have be used to detect such potentials, which typically have frequencies between 100-2000 Hz. Low frequency drift is also present, and might be due to breathing. Tests in the future could measure ECG drift as a function of breathing rate to confirm this hypothesis.

There is no easy way to remove absolutely all sources of noise. Therefore, the signal must be processed with digital filters. The raw ECG signal and PDS suggest the use of a 60 Hz bandstop to remove 60 Hz noise, a low pass filter to remove all other high frequency noise, and a high pass filter to remove drift.

The ability of a fourth order Butterworth bandstop at 58-62 Hz to reduce signal noise and remove the 60 Hz peak in the PDS (Figure 8) verifies the need for it in the digital analysis of an ECG. However, the resulting ECG signal is not clean and requires further high frequency filtering. Adding a Butterworth 30 Hz low pass filter can accomplish this (Figure 9). It is

important to note that using the wrong cut off frequency can have detrimental effects. To low of a cut off can significantly distorts the data, and make the signal look incomparable to a normal ECG. (Figure 10).

After all high frequency noise was removed, low frequency drift was still present in the baseline of the signal. A high pass filter was attempted to filter out this noise. However, all tries resulted in distortion of the baseline (Figure 11). Therefore, the development of optimal filter settings within this paper did not include a high pass filter. This most likely introduces some degree of error in biological measurements. It was accounted for in this report by taking clean ECGs. Future work should heavily focus on optimizing high pass filters.

4.4. Optimizing ECG High Pass Filter Settings

It is clear from the analysis above that proper filter settings are crucial for accurately improving an ECG signal (Figure 10). The NRSIQ method for optimizing low pass filters (Figure 12) was successful in identifying processing conditions which minimize noise while maintaining the height of the QRS complex. Graphs made for any order Butterworth or least-squares filter allow the experimenter to choose optimal low pass filter settings. For example, a signal noise graph for a fourth order low pass Butterworth filter shows that noise does not become significantly removed until a 30 Hz cutoff frequency is applied. However, the QRS does not significantly attenuate until cutoff frequencies of approximately 20 Hz are applied. Therefore, the optimal cut off frequency for a low pass fourth order Butterworth filter would be approximately 20 Hz because it maximizes signal height and minimized noise. Similar graphs made for least squares low pass filters (Figure 12) showed optimal cutoff frequencies of approximately 30 Hz (because noise is significantly reduced by a cutoff frequency of 40 Hz, and QRS amplitude does not significantly attenuate until the cutoff frequency equals 30 Hz). These graphs are significant, because they reduce the subjectivity of finding the “best” ECG filter settings by eye.

While these settings are considered optimal, they may introduce error into the analysis. Settings are chosen that maintain the highest QRS complex. However, this still includes a degree of attenuation that might cause loss of information. Furthermore, not all noise is removed. Noise at lower frequencies (like 15 Hz) cannot be distinguished from the ECG signal and therefore are not removed.

4.5. Use of Optimal ECG Collection Settings to Answer Physiological Topics

With the knowledge of how to optimally acquire and filter ECGs, we now have the ability to address important physiological topics. The first that may be considered are heart rate calculation and the effect of various activities on heart rate. A second is measuring the electrical axis of the heart.

4.5.1. Heart Rate Determination

The heart rates calculated via the peak detection method and PDS methods (78.0 ± 0.3 and 79.7 ± 0.9 bpm respectively) were found to be statistically different (P value ~ 0). The heart rate calculated by peak detection is considered to be the more accurate method because it is an actual measure of heart rate. The PDS analysis only infers the heart rate from frequencies found in the spectrum (Figure 13). In addition, the PDS analysis is a less accurate measure because the fundamental peak can be convoluted with any noise in the 1 Hz range.

Not only is the PDS method less accurate, it is impractical for use in most application. In order to obtain a 1 bpm resolution, the PDS window must be at least 1 minute long. When considering Welch averaging with at least four windows, a four minute recording is required to measure heart rate. This is impractical in most clinical, experimental or recreational settings where real-time data is desired. The peak detection method is therefore a far superior method and is used throughout the remainder of this report.

4.5.2. Effect of Activity on Heart Rate

As expected, exercise caused a substantial increase in heart rate for both subjects. This is caused by a higher need for oxygen in the muscles. The heart beats faster to deliver more oxygen. Ultimately, the increase was most likely due to a sympathetic response to physical exertion.

All ECGs taken while a subject performed the Valsalva maneuver showed the expected characteristic increases in heart rate (Figure 14). This confirms with what has been previously reported in the literature, and can be explained physiologically. Attempting to exhale without the nose or mouth open increases chest cavity pressure, which decreases venous return. In response, the heart increases contraction frequency to compensate. This is maintained until the maneuver is stopped, which equalizes the pressure.

4.5.3. Calculating Electrical Axis of the Heart

The two subjects mean QRS axis (55.1 ± 0.8 bpm and 53.6 ± 0.5 bpm) fall well within the range of what is deemed healthy by clinicians (-30 to +90^{o}). Therefore, the subjects have normal hearts (within the scope of this test).

The mean QRS calculated from the three different two-lead combinations were close, but not identical for each subject. An ANOVA test showed that the mean QRS calculated from the three different two-lead combinations were not statistically equivalent. Theoretically, all combinations should produce the same value. Modifications should be made to the equipment setup and filtering methods to determine the source of this error. However, until such additional tests can be performed, the best way to describe the mean QRS obtained from these methods is the average of all lead combinations.

5. Summary

ECGs can provide a lot of profound physiological information. However, in order to perform such analyses, optimal settings for sampling rate and filtering must be set. We were able to successfully develop methods to optimize such settings and maximize information

gained from ECGs. These settings were then successfully applied to determining how activities affect heart rate and measuring the mean electrical axis of the heart.

6. Works Cited

P. S. Hamilton and W. J. Tompkins, Quantitative investigation of QRS detection rules using the MIT/BIH arrhythmia database, IEEE Trans. Biomed. Eng., BME-33(12):1157-1165, 1986.

An algorithm for EMG noise detection in large ECG data. Raphisak, P. Schuckers, S.C. de Jongh Curry, A. Dept. of Comput. Sci. & Electr. Eng., West Virginia Univ., Morgantown, WV, USA;

Clinical utility of surface EMG: Report of the Therapeutics and Technology Assessment Subcommittee of the American Academy of Neurology S.L. Pullman, MD, FRCP(C); D.S. Goodin, MD; A.I. Marquinez, MD; S. Tabbal, MD; and M. Rubin, MD, FRCP(C)